Stem Cell Reports
Article
ISSCR
OPEN ACCESS

Srebf1c preserves hematopoietic stem cell function and survival as a switch of mitochondrial metabolism

Yukai Lu,[1,3] Zihao Zhang,[1,3] Song Wang,[1] Yan Qi,[1] Fang Chen,[1] Yang Xu,[1] Mingqiang Shen,[1] Mo Chen,[1] Naicheng Chen,[1] Lijing Yang,[1] Shilei Chen,[1] Fengchao Wang,[1] Yongping Su,[1] Mengjia Hu,[1,2,*] and Junping Wang[1,*]

[1]State Key Laboratory of Trauma, Burns and Combined Injury, Institute of Combined Injury, Chongqing Engineering Research Center for Nanomedicine, College of Preventive Medicine, Third Military Medical University, Gaotanyan Street 30, Chongqing 400038, China
[2]Chinese PLA Center for Disease Control and Prevention, No. 20 Dongda Street, Fengtai District, Beijing 100071, China
[3]These authors contributed equally
*Correspondence: weichen1111@yahoo.com (M.H.), wangjunp@yahoo.com (J.W.)
https://doi.org/10.1016/j.stemcr.2022.01.011

SUMMARY

Mitochondria are fundamental but complex determinants for hematopoietic stem cell (HSC) maintenance. However, the factors involved in the regulation of mitochondrial metabolism in HSCs and the underlying mechanisms have not been fully elucidated. Here, we identify sterol regulatory element binding factor-1c (*Srebf1c*) as a key factor in maintaining HSC biology under both steady-state and stress conditions. *Srebf1c* knockout (*Srebf1c*$^{-/-}$) mice display increased phenotypic HSCs and less HSC quiescence. In addition, *Srebf1c* deletion compromises the function and survival of HSCs in competitive transplantation or following chemotherapy and irradiation. Mechanistically, SREBF1c restrains the excessive activation of mammalian target of rapamycin (mTOR) signaling and mitochondrial metabolism in HSCs by regulating the expression of tuberous sclerosis complex 1 (*Tsc1*). Our study demonstrates that *Srebf1c* plays an important role in regulating HSC fate via the TSC1-mTOR-mitochondria axis.

INTRODUCTION

Hematopoietic stem cells (HSCs), which sit at the top of the hematopoietic hierarchy, can self-renew and differentiate into all kinds of blood cells over the lifespan (Carrelha et al., 2018; Pinho and Frenette, 2019). During the steady state, the majority of HSCs are retained in a specific bone marrow (BM) microenvironment and are maintained in a quiescent state (Cabezas-Wallscheid et al., 2017; Mendelson and Frenette, 2014). It has been well established that the loss of quiescence may impair the long-term repopulation capability of HSCs, eventually resulting in the perturbation of hematopoietic homeostasis (Hou et al., 2015). Previous studies have identified many cell-intrinsic and cell-extrinsic factors that are involved in regulating HSC function (Pinho and Frenette, 2019). In recent years, increasing attention has been focused on cell metabolism, such as mitochondrial metabolism, fatty acid oxidation, glutamine metabolism, and amino acid catabolism, in adult stem cells (Khoa et al., 2020; Ludikhuize et al., 2020; Tohyama et al., 2016; Villegas et al., 2019), but how metabolic changes affect the fate of HSCs remains incompletely understood.

In the hypoxic microenvironment, quiescent HSCs mainly use glycolysis to generate energy, which is required to preserve their self-renewal ability (Takubo et al., 2010, 2013). In response to various stress signals, anaerobic metabolism will switch to mitochondrial respiration to meet the energy demands for HSC proliferation (Wang et al., 2021). Previous studies reported that the mammalian target of rapamycin (mTOR), AMP kinase (AMPK), peroxisome proliferator-activated receptor-gamma coactivator 1α (PGC-1α), and Ca^{2+} play a central role in mitochondrial energy metabolism (Cantó et al., 2009; Cunningham et al., 2007; Umemoto et al., 2018). These pathways mediate the partial role of other factors, such as TSC-1, TWIST1, LKB1, Dlk1-Gtl2, SRC-3, and MEK1, in regulating HSC biology (Baumgartner et al., 2018; Chen et al., 2008; Gan et al., 2008, 2010; Hu et al., 2018; Qian et al., 2016; Wang et al., 2021). Despite considerable study, the exquisite modulation of mitochondrial metabolism is still incompletely characterized.

Sterol regulatory element binding factor-1c (*Srebf1c*; also called *SREBP1c/ADD1*) is one of the highly conserved basic helix-loop-helix-leucine zipper family members. It has been shown that *Srebf1c* is an indispensable metabolic regulator in both humans and mice (Wang et al., 2015). As a transcription factor, SREBF1c can control the expression of key enzymes for fatty acid synthesis, such as fatty acid synthase (FAS), acetyl coenzyme A (CoA) carboxylase 1 (ACC1), and stearoyl-CoA desaturase 1 (SCD1), in adipocytes and liver cells (Wang et al., 2015). In addition, *Srebf1c* was reported to repress fatty acid metabolism and mitochondrial function in peripheral nerve cells by regulating the expression of peroxisome proliferator-activated receptor α (Pparα) ligands (Cermenati et al., 2015). Interestingly, another study showed that *Srebf1c* modulates glucose metabolism in natural killer (NK) cells (Assmann et al., 2017). These findings indicate that *Srebf1c* functions in a

cell context-dependent manner. However, it is still unclear whether *Srebf1c* can regulate HSC function by affecting specific metabolic processes.

To elucidate the role of *Srebf1c* in HSCs, we used a *Srebf1c* knockout (*Srebf1c*$^{-/-}$) mouse model and found that loss of *Srebf1c* leads to significant proliferation and activation of phenotypic HSCs, accompanied by impairment in their hematopoietic reconstitution capacity. Mechanistically, SREBF1c inhibited the hyperactivation of the mTOR pathway and mitochondrial metabolism via transcriptional control of *Tsc1* expression. Overall, our study provides new insight into the role of *Srebf1c* in maintaining HSC function and survival by modulating the TSC1-mTOR-mitochondria axis.

RESULTS

Srebf1c is enriched in HSCs, and its deficiency slightly affects mature hematopoiesis in mice

To understand the role of *Srebf1c* in hematopoiesis, we analyzed its expression pattern in the BM of mice. Quantitative real-time-PCR analysis showed that *Srebf1c* expression was relatively higher in hematopoietic stem and progenitor cells (HSPCs), especially in long-term HSCs (LT-HSCs), than in lineage-positive (Lin$^+$) cells (Figure 1A). Then, a *Srebf1c*$^{+/LacZ}$ mouse model (Liang et al., 2002), which expresses the *lacZ* gene after *Srebf1c* deletion, was used in our study. Similar expression profiling was observed by flow cytometric analysis with fluorescein di-β-D-galactopyranoside (FDG) staining (Figure 1B). These findings suggest that *Srebf1c* may play a distinctive role in HSC biology. By analyzing *Srebf1c*$^{-/-}$ and their littermate wild-type (WT) control mice, we found that the depletion of *Srebf1c* resulted in splenomegaly with increased B cell numbers (Figures 1C–1F and S1A–S1C). However, other conventional hematopoietic parameters were largely unchanged after *Srebf1c* knockout (Figures 1G–1I and S1D). Thus, these data indicate that *Srebf1c* deficiency has only a slight effect on mature hematopoiesis.

Srebf1c deletion disturbs normal HSPC pool

To further acquire insight into the role of *Srebf1c* in hematopoiesis, we conducted flow cytometric analysis on the HSPC compartment. Deletion of *Srebf1c* significantly increased the percentage and absolute number of Lin$^-$ Sca1$^+$ c-Kit$^+$ cells (LSKs), but not myeloid progenitors (MPs), in the BM (Figures 2A and 2B). We then examined the LSK subpopulation and observed that despite the unbalanced proportion of LT-HSCs, short-term HSCs (ST-HSCs), and multipotent progenitors (MPPs), the absolute number of all of the subpopulations was increased after *Srebf1c* deficiency (Figures 2C and 2D). Similar results were obtained using another combination of HSC markers, CD48 and CD150 (Figures 2E and 2F). In addition, *Srebf1c*$^{-/-}$ mice showed an increased number of megakaryocyte-erythroid progenitors (MEPs) but a decreased number of common myeloid progenitors (CMPs) in the BM (Figures 2G and 2H). In contrast, no significant alteration was observed in the number of granulocyte-macrophage progenitors (GMPs) or common lymphoid progenitors (CLPs) when Srebf1c was deleted (Figures 2G and 2H). Consistent with the HSC expansion in the BM, a marked increase in LSK number was found in the spleen and peripheral blood (PB) of *Srebf1c*-null mice (Figures 2I and S2). However, we observed increased numbers of MEPs and CLPs in the spleens of *Srebf1c*$^{-/-}$ mice (Figure 2J). Thus, *Srebf1c* is required to sustain a normal HSPC pool in mice.

Srebf1c knockout leads to the loss of HSC quiescence

To determine whether *Srebf1c* deficiency affects HSC cell-cycle status, we performed Ki67 and Hoechst 33342 staining. Flow cytometric analysis revealed that the frequency of HSCs in G0 phase was reduced and the frequency in G1 and S/G2/M phases was increased in *Srebf1c*$^{-/-}$ mice (Figures 3A–3C and S3A). Consistently, the bromodeoxyuridine (BrdU) incorporation assay showed that *Srebf1c* deficiency promoted the proliferation of HSCs (Figures 3D and S3B). Next, quantitative real-time-PCR analysis showed that the expression of cell-cycle inhibitors, such as *Cdkn1a* and *Cdkn1c*, was downregulated, whereas the expression of *Ccnb1*, *Ccne1*, and *Cdk2* was upregulated in *Srebf1c*$^{-/-}$ HSCs (Figure 3E). Proliferative active cells are more sensitive to genetic insults, such as ionizing radiation (IR) and chemotherapy (Sinha et al., 2019; Wang et al., 2016). As expected, *Srebf1c*$^{-/-}$ mice displayed reduced survival compared with WT mice following sequential 5-fluorouracil (5-FU) treatment (Figure 3F) or a lethal dose of total body irradiation (Figure 3G). Furthermore, annexin V and 7-aminoactinomycin D (7-AAD) staining showed an increased apoptosis rate in *Srebf1c*$^{-/-}$ HSCs (Figures 3H and S3C). Collectively, *Srebf1c* knockout drives the proliferation and accelerates the apoptosis of HSCs.

Srebf1c deficiency compromises the hematopoietic reconstitution ability of HSCs

To investigate whether deletion of *Srebf1c* affects HSC function, we conducted a homing assay and found that the homing efficiency was comparable between WT and *Srebf1c*$^{-/-}$ HSCs (Figure S4A). Then, we performed serial competitive BM transplantation (BMT) assays (Figure 4A). The percentages of *Srebf1c*$^{-/-}$ donor-derived cells were significantly reduced in recipients' PB after primary and secondary BMT, accompanied by a defect in long-term

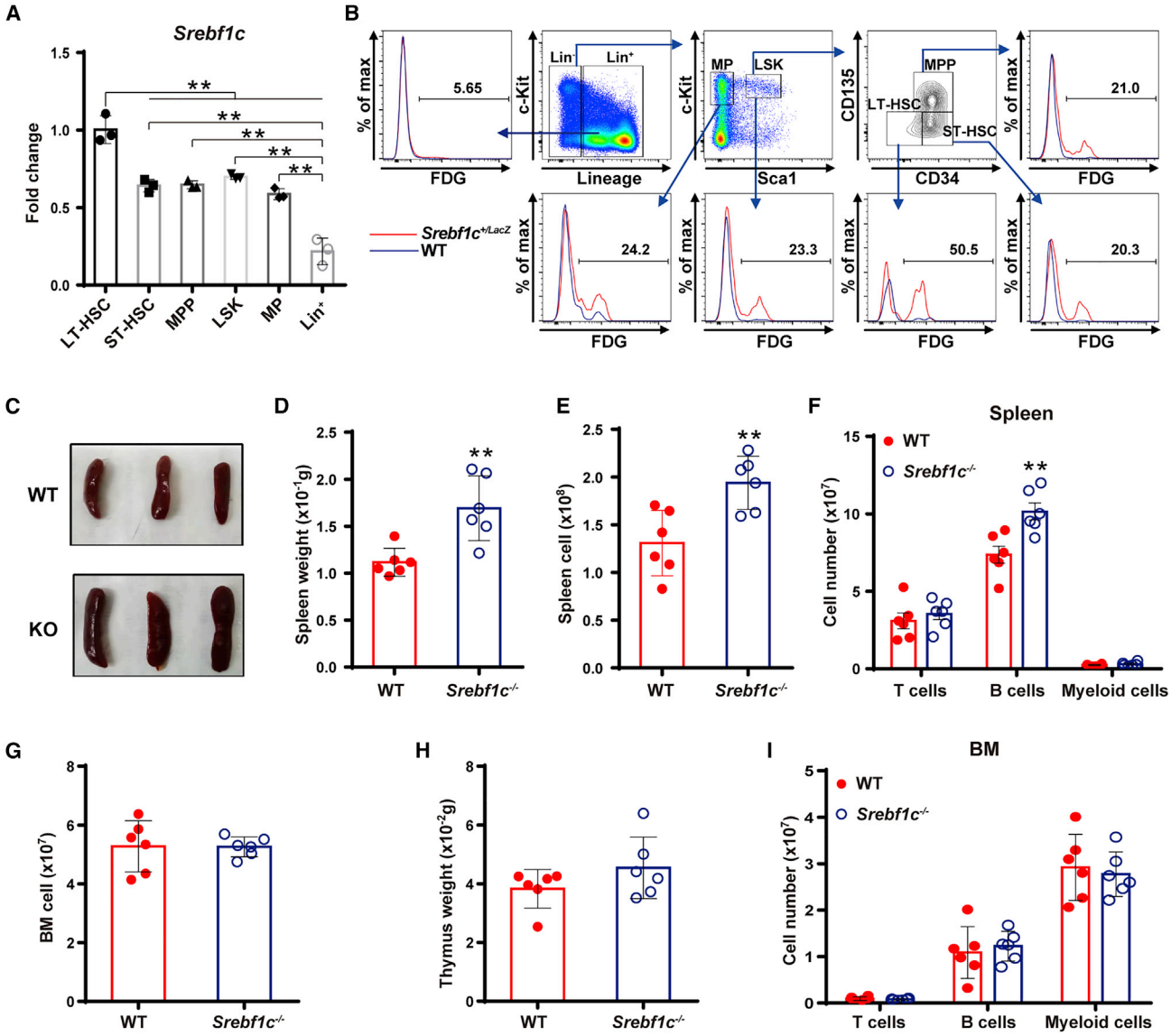

Figure 1. *Srebf1c* is enriched in HSCs, and its deficiency slightly affects mature hematopoiesis in mice

(A) Relative expression levels of *Srebf1c* in long-term HSCs (LT-HSCs), short-term HSCs (ST-HSCs), multipotent progenitors (MPPs), LSKs, myeloid progenitors (MPs), and lineage-positive (Lin^+) cells sorted from normal WT mice were detected by quantitative real-time-PCR (n = 3). The gating strategies are shown in Figure S1A.

(B) Flow cytometric analysis with FDG staining to detect *Srebf1c* expression in LT-HSCs, ST-HSCs, MPPs, LSKs, MPs, and Lin^+ cells from WT and $Srebf1c^{+/LacZ}$ mice (n = 3).

(C–F) Spleen parameters, including (C) size, (D) weight, (E) total cell number, and (F) mature cell numbers (T cells, B cells, and myeloid cells) in WT and $Srebf1c^{-/-}$ mice (n = 3–6).

(G and H) Total BM cell number of 2 femurs and tibias (G) and thymus weight (H) in WT and $Srebf1c^{-/-}$ mice (n = 6).

(I) T cell, B cell, and myeloid cell numbers in the BM of WT and $Srebf1c^{-/-}$ mice (n = 6). **p < 0.01.

multilineage reconstitution (Figures 4B–4E). Consistently, $Srebf1c^{-/-}$ HSCs formed significantly fewer colonies *in vitro* than WT HSCs (Figure S4B). As *Srebf1c* was globally deleted in mice, we performed reciprocal BMT assays to assess how *Srebf1c* regulates HSC biology (intrinsic and/or extrinsic) (Figures 4F and 4I). Consistent with the phenotype of HSCs in *Srebf1c*-null mice, recipients transplanted with $Srebf1c^{-/-}$ BM cells showed increased HSC numbers and proliferation (Figures 4G, 4H, and S4C). In contrast, no significant difference in HSC phenotype was observed

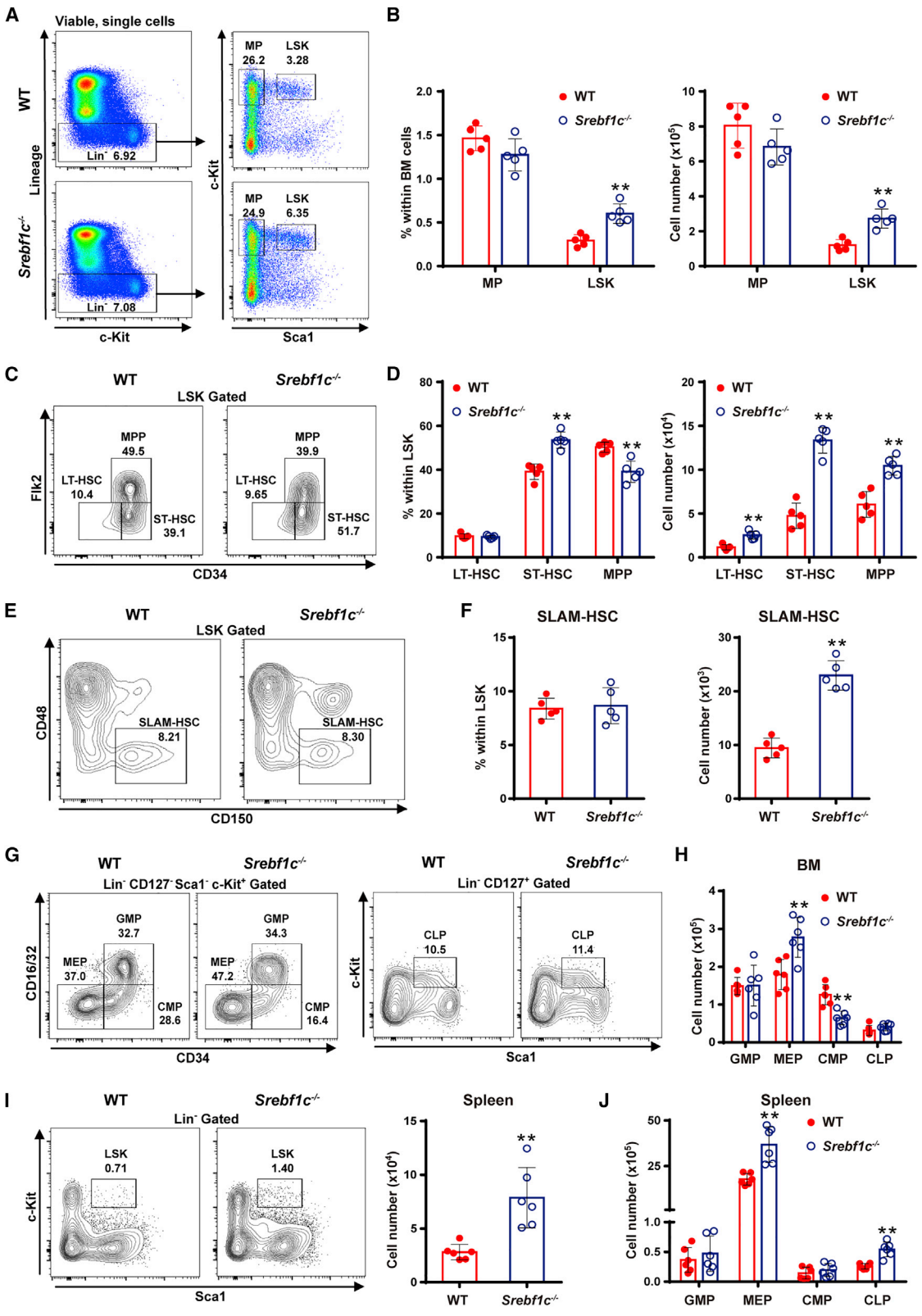

(legend on next page)

between WT and *Srebf1c*$^{-/-}$ mice that received CD45.1 BM cells (Figures 4J, 4K, and S4D). These results suggest that *Srebf1c* is required for maintaining HSC long-term repopulation possibly in a cell-intrinsic manner.

Srebf1c ablation leads to significantly increased mitochondrial metabolism in HSCs

To further explore the underlying mechanism by which *Srebf1c* regulates HSC quiescence and function, we conducted RNA sequencing (RNA-seq) using LSKs from WT and *Srebf1c*$^{-/-}$ mice. Bioinformatics analysis showed that 595 genes were upregulated and 1,542 genes were downregulated in *Srebf1c*$^{-/-}$ LSKs relative to WT controls (Figures 5A and 5B). Notably, the upregulated genes were significantly enriched in metabolic pathways (Figure 5C). Subsequently, we performed gene set enrichment analysis (GSEA) and found that proliferation-related HSC signatures were enriched in *Srebf1c*$^{-/-}$ HSCs, while quiescence-related signatures were enriched in WT HSCs (Figures 5D and S5A), consistent with the above findings. Although previous studies reported that *Srebf1c* regulates lipid synthesis (Wang et al., 2015), the expression of two key enzymes in this pathway was not significantly altered in HSCs following *Srebf1c* deficiency (Figure S5B). Interestingly, *Srebf1c*-deleted HSCs presented a significant upregulation of metabolic signatures, including the citrate cycle, carbon metabolism, oxidative phosphorylation, and mitochondrial organization compared to WT cells (Figure 5E). It has been shown that cell proliferation is always associated with a large cell size and active metabolism (Suda et al., 2011). HSCs from *Srebf1c*$^{-/-}$ mice showed a larger cell size (Figure S5C). Given that mitochondria play a central role in energy metabolism, which is closely associated with hematopoietic homeostasis (Liang et al., 2020; Mansell et al., 2021; Wang et al., 2021), we then measured the mitochondrial properties of HSCs. Mitochondrial mass, membrane potential, and the expression of mitochondria-related genes, such as *Cyc1*, *Atp4a*, *Cox5a*, *Cox6a2*, *Ndufc1*, and *Idh3a*, were increased in *Srebf1c*-null HSCs (Figures 5F, 5G, and S5D–S5G). Notably, mitochondrial metabolism was comparable between WT and *Srebf1c*$^{-/-}$ MPs (Figures 5F and 5G), revealing that *Srebf1c* may play a unique role in HSCs (to a greater extent in LSKs). In addition, transmission electron microscopy (TEM) revealed that mitochondrial number and folds of cristae were increased in *Srebf1c*$^{-/-}$ HSCs (Figure 5H). Furthermore, we observed increased glucose uptake, oxygen consumption rate (OCR), and pyruvate dehydrogenase (PDH) activity in *Srebf1c*$^{-/-}$ HSCs (Figures 5I, S5H, and S5I), accompanied by elevated ATP and reactive oxygen species (ROS) levels (Figures 5K and 5L). In contrast, decreased extracellular acidification rate (ECAR), lactate dehydrogenase (LDH) activity, and pyruvate and lactate levels were found in *Srebf1c*$^{-/-}$ HSCs (Figures 5J, 5M, S5J, and S5K). Overall, these data suggest that *Srebf1c* maintains HSC function by suppressing mitochondrial activity.

SREBF1c inhibits the hyperactivation of mTOR signaling via the transcriptional control of *Tsc1*

mTOR signaling plays a critical role in regulating mitochondrial metabolism and HSC maintenance (Liu et al., 2019; Qian et al., 2016). Notably, a markedly enriched mTOR complex 1 (mTORC1) signaling in *Srebf1c*$^{-/-}$ HSCs was observed in our GSEA data (Figure 6A). To further verify whether the mTOR pathway is activated in *Srebf1c*$^{-/-}$ HSCs, we examined the key points of this pathway. As anticipated, the phosphorylation levels of mTOR, S6, and 4E-BP1 and the expression of PGC-1α, a master regulator of mitochondrial metabolism, were significantly increased in HSCs after *Srebf1c* deletion (Figures 6B–6D and S6A). Akt is an upstream activator of mTOR, but the level of p-Akt was not altered in HSCs in the absence of *Srebf1c* (Figure S6B).

Figure 2. *Srebf1c* deletion disturbs normal HSPC pool

(A) Representative flow cytometric plots of the percentage of HSPCs in WT and *Srebf1c*$^{-/-}$ BM.

(B) The percentage (left) and absolute number (2 femurs and tibias; right) of MPs and LSKs in the BM from WT and *Srebf1c*$^{-/-}$ mice (n = 5).

(C) Representative flow cytometric plots of the percentage of HSC subpopulations in WT and *Srebf1c*$^{-/-}$ LSKs.

(D) The percentage of subpopulations in LSKs (left) and the absolute number (2 femurs and tibias) of LT-HSCs, ST-HSCs, and MPPs in the BM (right) of WT and *Srebf1c*$^{-/-}$ mice (n = 5).

(E) Representative flow cytometric plots of the percentage of signaling lymphocyte activation molecule (SLAM)-HSCs (CD150^{+} CD48^{-} LSKs) in WT and *Srebf1c*$^{-/-}$ LSKs.

(F) The percentage of SLAM-HSCs in LSKs (left) and the absolute number (2 femurs and tibias) of SLAM-HSCs in the BM (right) of WT and *Srebf1c*$^{-/-}$ mice (n = 5).

(G) Representative flow cytometric plots of the percentage of GMPs, MEPs, CMPs (left), and CLPs (right) in the BM of WT and *Srebf1c*$^{-/-}$ mice.

(H) The absolute number (2 femurs and tibias) of GMPs, MEPs, CMPs, and CLPs from WT and *Srebf1c*$^{-/-}$ BM (n = 6).

(I) Representative flow cytometric plots of the percentage of splenic LSKs (left) and the absolute number of LSKs in the spleens (right) of WT and *Srebf1c*$^{-/-}$ mice (n = 6).

(J) The absolute number of GMPs, MEPs, CMPs, and CLPs in the spleens of WT and *Srebf1c*$^{-/-}$ mice (n = 6).

**$p < 0.01$.

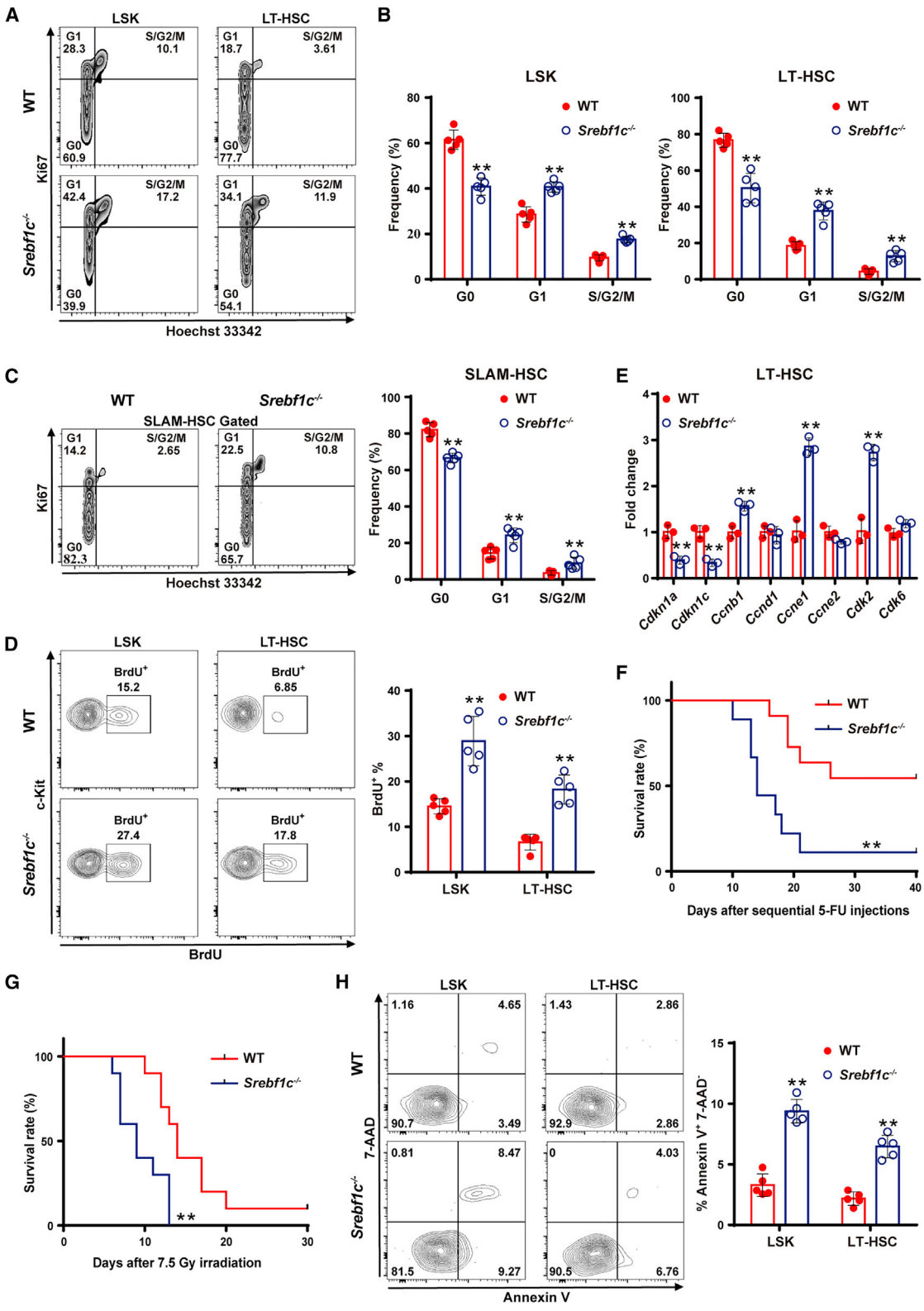

(legend on next page)

However, studies have shown that mTOR signaling is negatively regulated by tuberous sclerosis proteins 1 and 2 (TSC1/2) (Hay, 2005; Lee et al., 2007). In fact, the mRNA and protein levels of TSC1, but not TSC2, were lower in *Srebf1c*$^{-/-}$ HSCs than in control cells (Figures 6E–6G and S6C–S6E). Moreover, we noticed that *Srebf1c*$^{-/-}$ mice exhibited HSC phenotypes similar to those of *Tsc1*$^{-/-}$ mice (Chen et al., 2008; Gan et al., 2008). Therefore, we speculated that SREBF1c restricts mTOR activity and mitochondrial metabolism in HSCs by modulating TSC1 expression (Figure 6H). Subsequently, bioinformatic prediction revealed that there was a potential binding site of SREBF1c in the *Tsc1* promoter region (Figure 6I), which was further confirmed by chromatin immunoprecipitation (ChIP) assays (Figure 6J). These results demonstrate that SREBF1c suppresses mTOR signaling and downstream mitochondrial metabolism by directly controlling the transcription of *Tsc1*.

Inhibition of mTOR activation or scavenging ROS improves HSC defects in *Srebf1c*-deleted mice

To further determine whether hyperactivation of the mTOR pathway is responsible for HSC defects, *Srebf1c*$^{-/-}$ mice were administered the mTORC1 inhibitor rapamycin. We found that rapamycin treatment significantly inhibited mTOR activity, mitochondrial mass, mitochondrial membrane potential, glucose uptake, and ROS production in *Srebf1c*-null HSCs (Figures 7A–7G andS7A). In addition, phenotypic expansion and aberrant proliferation of HSCs in *Srebf1c*$^{-/-}$ mice were largely reversed after rapamycin treatment (Figures 7H, 7I, and S7B). Inhibition of mTOR activity by rapamycin significantly rescued the impaired function of *Srebf1c*$^{-/-}$ HSCs (Figures 7J and S7C). Finally, to confirm whether the elevated ROS levels caused by mitochondrial activation contribute to HSC defects in *Srebf1c*$^{-/-}$ mice, the effective ROS scavenger *N*-acetyl-L-cysteine (NAC) was applied (Figure S7D). We found that NAC treatment partially reversed the phenotypic and functional defects of *Srebf1c*-deficient HSCs (Figures S7E–S7I). Our data demonstrate that *Srebf1c* maintains HSC homeostasis via the limitation of mTOR activation and mitochondrial metabolism (Figure 7K).

DISCUSSION

HSC homeostasis needs to be exquisitely regulated for the replenishment of all blood cells under both steady-state and stress conditions (Mendelson and Frenette, 2014; Pinho and Frenette, 2019). It has been reported that transcription factors, epigenetic factors, multiple RNAs (microRNAs, long-length noncoding RNAs, circular RNAs), and cytokines participate in the modulation of HSC biology (Hou et al., 2015; Hu et al., 2021; Li et al., 2018; Qian et al., 2016; Xia et al., 2018; Yamashita and Passegue, 2019). Notably, energy metabolism is emerging as a regulatory element of HSC maintenance, whereas the underlying mechanism remains elusive. Here, we reported for the first time that SREBF1c inhibits the mTOR pathway and downstream mitochondrial metabolism by regulating the transcription of *Tsc1*, which is required for promoting HSC maintenance in mice.

The Srebfs family, including *Srebf1a*, *Srebf1c*, and *Srebf2* isoforms, displays incompletely overlapping functions for regulating several metabolic processes (Wang et al., 2015). For example, *Srebf2* and *Srebf1a* can participate in cholesterol biosynthesis, while *Srebf1c* preferentially governs lipogenesis (Liang et al., 2002). Cholesterol-induced *Srebf2* activation promotes HSPC expansion in atherosclerotic cardiovascular disease in zebrafish (Gu et al., 2019). However, less attention has been focused on the role of *Srebf1c* in hematopoiesis. In the present study, we showed that *Srebf1c* is relatively enriched in HSCs in the hematopoietic system, suggesting that *Srebf1c* may participate in the regulation of HSC behavior. Using a *Srebf1c*$^{-/-}$ mouse model, we found that *Srebf1c* deficiency leads to an expansion of

Figure 3. *Srebf1c* knockout leads to the loss of HSC quiescence

(A) Representative flow cytometric plots of cell-cycle distribution of LSKs and LT-HSCs from WT and *Srebf1c*$^{-/-}$ mice by Ki67/Hoechst 33342 staining.

(B) The frequency of LSKs (left) and LT-HSCs (right) in G0, G1, and S/G2/M phases of WT and *Srebf1c*$^{-/-}$ mice (n = 5).

(C) Flow cytometric analysis of cell-cycle distribution of SLAM-HSCs from WT and *Srebf1c*$^{-/-}$ mice (n = 5).

(D) Representative flow cytometric plots of cell proliferation with BrdU staining (left) and the proportion of BrdU^{+} cells (right) in LSKs and LT-HSCs of WT and *Srebf1c*$^{-/-}$ mice (n = 5).

(E) The relative expression levels of cell-cycle-related genes in LT-HSCs sorted from WT and *Srebf1c*$^{-/-}$ mice were measured by quantitative real-time-PCR (n = 3).

(F and G) Kaplan-Meier survival analysis of WT and *Srebf1c*$^{-/-}$ mice following (F) sequential 5-FU administration and (G) 7.5 Gy irradiation (n = 9–10).

(H) Representative flow cytometric plots of apoptosis with annexin V/7-AAD staining (left) and the percentage of annexin V^{+} 7-AAD^{-} cells (right) in LSKs and LT-HSCs from WT and *Srebf1c*$^{-/-}$ mice (n = 5).

**$p < 0.01$.

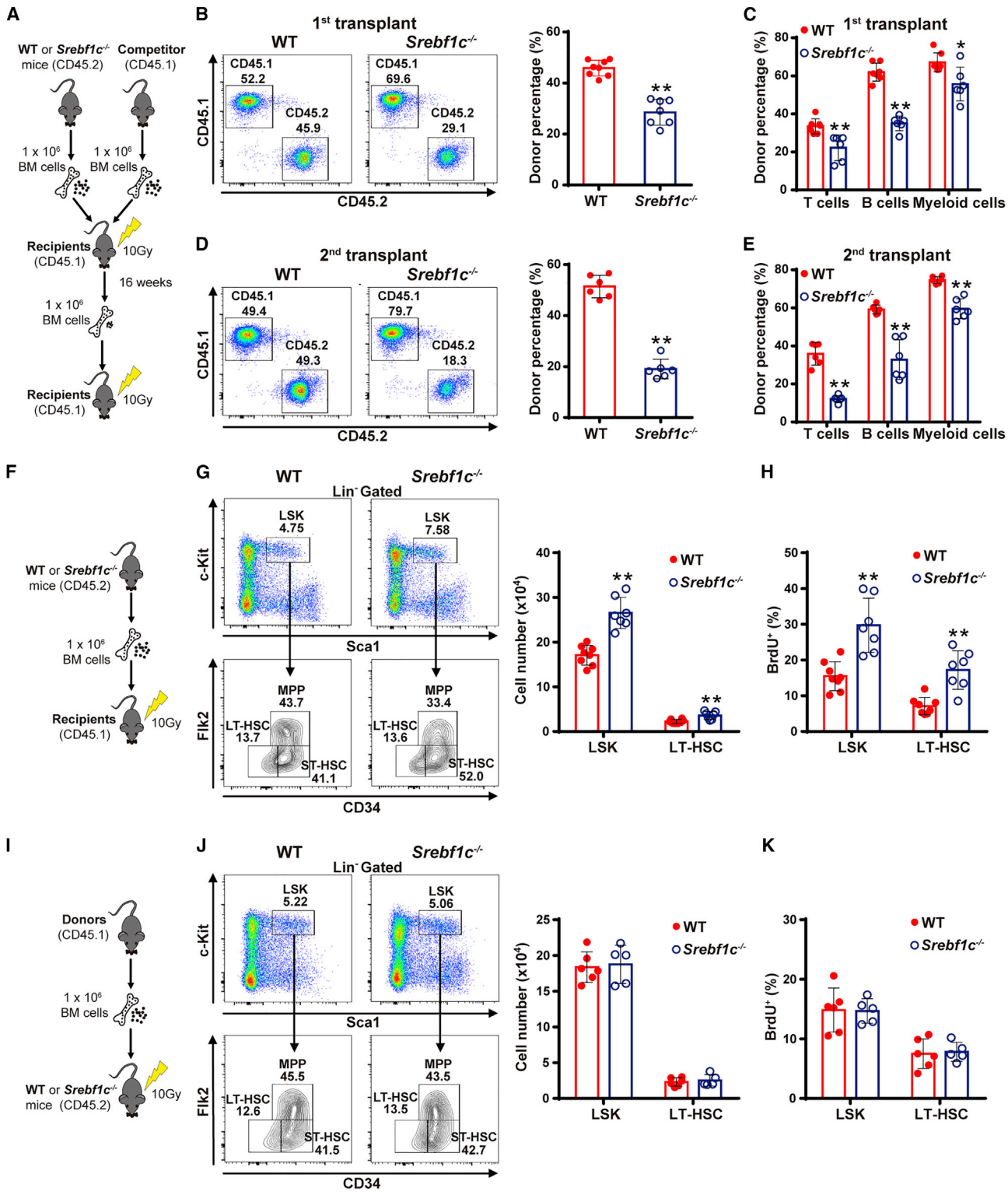

Figure 4. Loss of *Srebf1c* compromises the long-term reconstitution ability of HSCs

(A) Schematic for competitive transplantation with WT and *Srebf1c*$^{-/-}$ BM cells.

(B–E) Flow cytometric analysis of the donor percentages (B and D) and multilineage (T cells, B cells, myeloid cells) reconstitution (C and E) in the PB of CD45.1^{+} recipient mice at 16 weeks after the first (B and C) and second (D and E) transplantations (n = 6–8).

(legend continued on next page)

phenotypic HSCs in the BM. In addition, increased HSPC and mature cell numbers in the spleen, accompanied by an enlarged spleen, were observed in *Srebf1c*$^{-/-}$ mice, implying that the loss of *Srebf1c* may promote extramedullary hematopoiesis. In the steady state, HSCs with robust self-renewal potency are in a quiescent state. This property can protect HSCs from stress-induced injury and prevent their premature aging and exhaustion during long-term hematopoietic output (Takubo et al., 2010; Wang et al., 2021). Previous studies have shown that *Srebf1c* maintains the quiescence of hepatic satellite cells, but promotes the proliferation of pancreatic β cells (Lee et al., 2019; Su et al., 2020). In our study, we observed that the deletion of *Srebf1c* significantly impaired HSC quiescence, resulting in increased sensitivity to 5-FU and irradiation and decreased long-term repopulation capacity. HSC biology is co-regulated by cell-intrinsic or -extrinsic regulators in the BM niche (Pinho and Frenette, 2019). In our study, *Srebf1c* is globally deleted in mice. Although the reciprocal BMT assays and the *in vitro* colony-forming assay suggest that the defective function of *Srebf1c*$^{-/-}$ HSCs is probably cell intrinsic, we could not rule out the possibility of engraftment defect, developmental effects, or delayed environmental effect. To bring a deeper understanding of mechanism, a conditional knockout mouse model would be better.

Our previous studies and others have indicated that mitochondria emerge as drivers of HSC fate (Hu et al., 2018; Wang et al., 2021). Active mitochondrial metabolism is not compatible with quiescent HSCs, which mainly rely on glycolysis for energy production (Takubo et al., 2013). It has been reported that *Srebf1c* is involved in multiple metabolic processes, including lipid synthesis, fatty acid catabolism, and glycolysis (Wang et al., 2015), whereas whether *Srebf1c* regulates energy metabolism in HSCs remains unknown. Here, we showed that *Srebf1c* deletion results in a markedly increased mitochondrial function in HSCs, accompanied by elevated ROS levels. However, HSC impairment may be uncoupled from ROS elevation caused by mitochondrial abnormalities in some circumstances (Filippi and Ghaffari, 2019). In our study, scavenging ROS by NAC treatment partially rescued the defects of *Srebf1c*-null HSCs. These results demonstrate that elevated ROS levels induced by mitochondrial activation may be an important factor for HSC impairment in *Srebf1c*$^{-/-}$ mice.

mTOR is a serine/threonine kinase that exists in two complexes, mTORC1 and mTORC2 (Saxton and Sabatini, 2017). It is known that mTORC1, sensitive to rapamycin, participates in cell growth, mRNA translation, and protein synthesis (Inoki et al., 2002). In contrast, mTORC2 is insensitive to rapamycin, regulating cell survival, cytoskeleton organization, and gluconeogenesis (Hagiwara et al., 2012; Jacinto et al., 2004). Specifically, mTORC1 also controls mitochondrial biogenesis and activity by 4E-BP-dependent translational regulation or activating PGC-1α (Cunningham et al., 2007; Morita et al., 2013). Interestingly, either inhibition or activation of mTORC1 impairs HSC quiescence and hematopoietic potential (Ghosh et al., 2016; Kalaitzidis et al., 2012), suggesting that mTORC1 activity should be exquisitely regulated. Here, our findings revealed that the loss of *Srebf1c* leads to the hyperactivation of mTORC1 signaling and increased downstream protein levels in HSCs. As a result, rapamycin treatment largely corrected the increased mitochondrial activity and rescued the defective quiescence and function of *Srebf1c*$^{-/-}$ HSCs, suggesting that the hyperactive mTORC1 and mitochondrial metabolism may occur earlier than HSC proliferation and impairment. Overall, we demonstrate that *Srebf1c* maintains HSC homeostasis mainly by limiting the activity of mTORC1 signaling.

Researchers have reported that Akt plays a central role in the activation of the mTORC1 pathway (Hay, 2005; Qian et al., 2016). However, no significant difference in p-Akt levels was observed between WT and *Srebf1c*$^{-/-}$ HSCs, suggesting that *Srebf1c* deficiency-induced mTORC1 activation is not mediated by increased Akt activity. In addition, TSC1 and TSC2 are recognized as suppressing mTORC1 activity in many tissues (Hay, 2005; Lee et al., 2007). Previous studies reported that *Tsc1* deletion increases HSC proliferation due to the abnormal activation of the mTORC1 pathway, leading to short-term expansion but loss of long-term hematopoietic function (Chen et al., 2008; Gan et al., 2008). Interestingly, the phenotypes of HSCs were comparable between *Srebf1c*$^{-/-}$ and *Tsc1*$^{-/-}$ mice. Both the mRNA and protein levels of TSC1 were significantly reduced after *Srebf1c* deletion. Furthermore, ChIP assays revealed that SREBF1c controls the transcription of *Tsc1* by directly binding to its promotor region. Although TSC1 and TSC2 are homologous proteins, little is known about the role of TSC2 in HSCs. Moreover, our study showed that the expression of TSC2 was not altered in HSCs following *Srebf1c* ablation. *Srebf1c* is well known to regulate the expression of many lipid metabolism-related target genes, such as *Fasn* and *Acc1* (Wang et al., 2015).

(F and I) Schematic for reciprocal transplantation.
(G–K) The absolute number (2 femurs and tibias) of LSKs and LT-HSCs and the frequency of BrdU incorporation in LSKs and LT-HSCs from (G and H) recipient mice (CD45.1) injected with 1 × 10^6 WT or *Srebf1c*$^{-/-}$ BM cells (n = 7–8) or (J and K) recipient mice (WT or *Srebf1c*$^{-/-}$; CD45.2) transplanted with 1 × 10^6 CD45.1 BM cells at 16 weeks after transplantation (n = 5–6).
*p < 0.05, **p < 0.01.

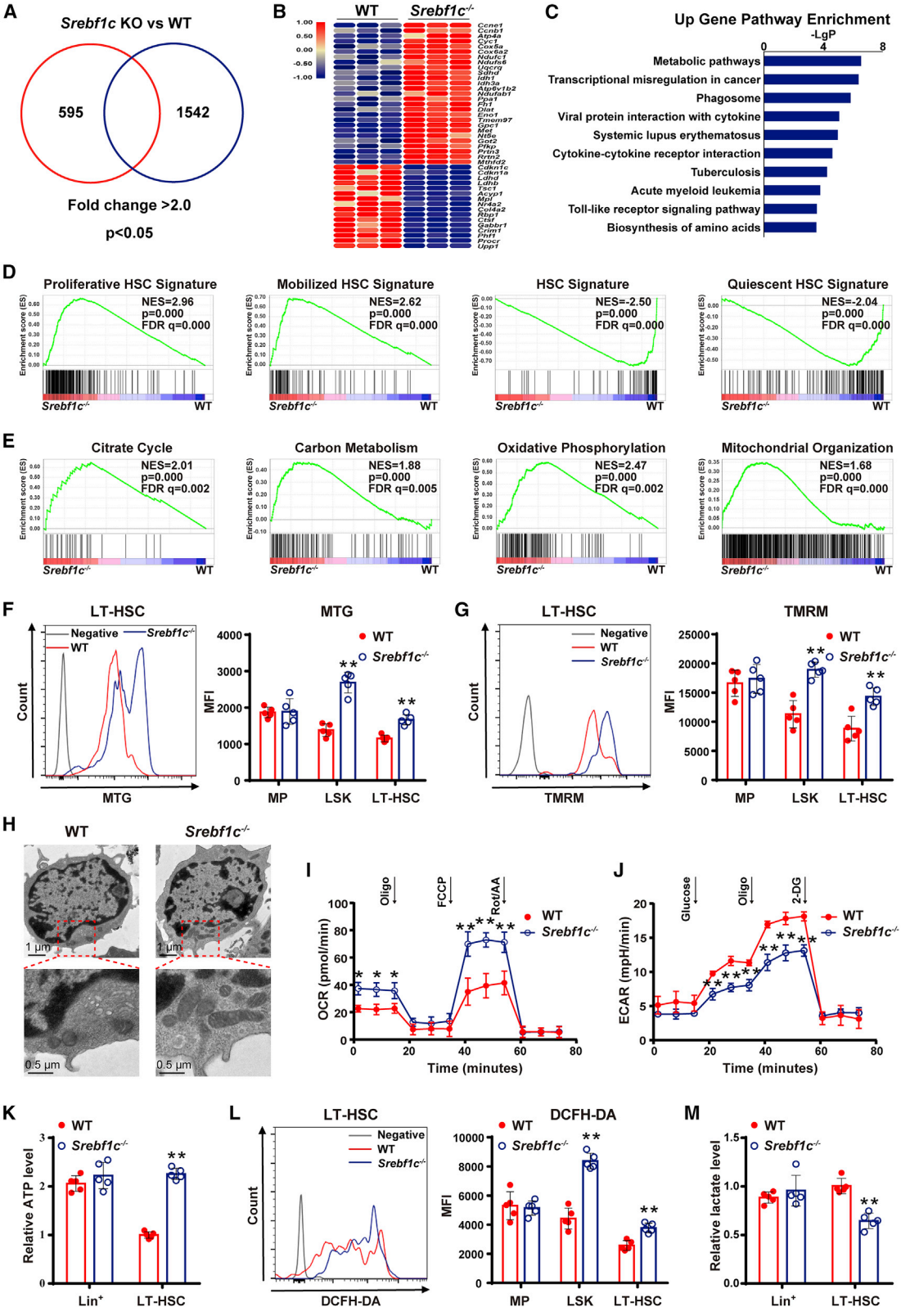

(legend on next page)

However, we did not observe any changes in *Fasn* and *Acc1* expression in *Srebf1c*$^{-/-}$ HSCs. However, previous studies reported that SREBF1c acts downstream of mTORC1 to facilitate lipid biosynthesis in liver and Schwann cells (Norrmen et al., 2014; Yecies et al., 2011). Combined with these findings, we reasonably speculate that there may be a negative feedback loop between SREBF1c and mTORC1, which controls the metabolic balance in HSCs.

In conclusion, our study demonstrates that *Srebf1c* plays an important role in orchestrating HSC fate via restriction of the hyperactivation of mTORC1 activity and mitochondrial metabolism by regulating *Tsc1* transcription. These findings improve our understanding of HSC biology and will give rise to novel avenues to facilitate HSC maintenance.

EXPERIMENTAL PROCEDURES

Mice

C57BL/6J mice were purchased from the Institute of Zoology (Chinese Academy of Sciences, Beijing, China). *Srebf1c*$^{-/-}$ mice were obtained from the Jackson Laboratory (Bar Harbor, ME, USA), and littermate WT mice served as controls. B_6 SJL mice (CD45.1) were a kind gift from Prof. Jinyong Wang (Guangzhou Institutes of Biomedicine and Health, Chinese Academy of Science, Guangzhou, China). All of the mice used were 8–10 weeks old. The animal experiments were performed according to the experimental procedures approved by the Animal Care Committee of the Third Military Medical University (Chongqing, China).

Flow cytometric analysis and sorting

Single-cell suspensions of mouse BM, spleen, and PB samples were prepared as we described previously (Hu et al., 2018, 2021). For hematopoietic cell phenotype analysis, cells were stained with antibodies identifying the following surface markers: Sca-1, c-Kit, CD34, Flk2, CD150, CD48, CD127, CD16/32, Gr-1, Mac-1, B220, CD3e, CD45.1, CD45.2, and the lineage cocktail (CD3e, Mac-1, Gr-1, B220, and Ter-119). Apoptosis, cell cycle, BrdU incorporation assay, and intracellular staining were performed as we described previously (Hu et al., 2018, 2021). All monoclonal antibodies (mAbs) were purchased from eBioscience (San Diego, CA, USA) or BioLegend (San Diego, CA, USA). Samples were detected by flow cytometry using a FACSVerse (BD Biosciences, San Jose, CA, USA) or FACSFortessa (BD Biosciences) and the data were analyzed using FlowJo 10.0 software (TreeStar, San Carlos, CA, USA).

For HSPC sorting, BM cells were first enriched by a Direct Lineage Cell Depletion Kit (Miltenyi Biotec, Bergisch Gladbach, Germany) following the manufacturer's instructions. Then, enriched Lin$^-$ cells were stained with the above surface markers. 4′,6-Diamidino-2-phenylindole (DAPI; Sigma, St. Louis, MO, USA) and trypan blue (Thermo Fisher Scientific, Grand Island, NY, USA) were used to confirm cell viability. Samples were sorted by a FACSAria II or FACSAria III sorter (BD Biosciences). Further details of flow cytometric antibodies are provided in Table S1.

Transplantation assays

The homing assay was performed as previously described (Gu et al., 2016). Briefly, 2×10^4 LSKs isolated from WT or *Srebf1c*$^{-/-}$ mice (CD45.2) were transplanted into lethally irradiated (10 Gy) CD45.1$^+$ mice. After 16 h, the homing efficiency was analyzed by flow cytometry. For competitive transplantation assays, 1×10^6 BM cells from WT or *Srebf1c*$^{-/-}$ mice (CD45.2) along with an equivalent number of CD45.1$^+$ BM cells were injected intravenously into recipient mice (CD45.1) after lethal irradiation (10 Gy). At 16 weeks after transplantation, the recipient mice (CD45.1/CD45.2) from the first transplantation were euthanized and then 1×10^6 BM cells were transplanted into new lethally irradiated (10 Gy) recipients (CD45.1). The chimerism level in the PB of the recipient mice was measured at the indicated time after transplantation. For reciprocal transplantation assays, 1×10^6 BM cells from WT or *Srebf1c*$^{-/-}$ mice (CD45.2) were transplanted into lethally irradiated (10 Gy) recipients (CD45.1), and 1×10^6 BM cells from CD45.1 mice were transplanted into lethally irradiated (10 Gy) WT or *Srebf1c*$^{-/-}$ recipients (CD45.2). At 16 weeks after transplantation, HSC phenotypes in the recipient mice were detected by flow cytometry.

Figure 5. *Srebf1c* ablation leads to significantly increased mitochondrial activity and metabolism in HSCs

(A–E) Transcriptomic profiling of WT and *Srebf1c*$^{-/-}$ LSKs.

(A) Venn diagram of the upregulated gene number (red box) and the downregulated gene number (blue box) in LSKs after *Srebf1c* deletion.

(B) Heatmap analysis of representative differentially expressed genes between WT and *Srebf1c*$^{-/-}$ LSKs.

(C) KEGG enrichment analysis of upregulated genes in LSKs after *Srebf1c* deletion. Listed are the top 10 enriched pathways.

(D and E) GSEA of (D) HSC-related signatures (proliferation, mobilization, and quiescence) and (E) metabolism-related signatures (citrate cycle, carbon metabolism, oxidative phosphorylation, and mitochondrial organization) in the RNA-seq data from WT and *Srebf1c*$^{-/-}$ LSKs

(F) Flow cytometric analysis of mitochondrial mass in MPs, LSKs, and LT-HSCs from WT and *Srebf1c*$^{-/-}$ mice by MTG staining (n = 5).

(G) Flow cytometric analysis of mitochondrial membrane potential in MPs, LSKs, and LT-HSCs from WT and *Srebf1c*$^{-/-}$ mice by TMRM staining (n = 5).

(H) Representative transmission electron microscopy (TEM) images of mitochondria morphology in LSKs from WT and *Srebf1c*$^{-/-}$ BM.

(I and J) Seahorse analysis of the (I) oxygen consumption rate (OCR) and (J) extracellular acidification rate (ECAR) in WT and *Srebf1c*$^{-/-}$ LSKs (n = 3).

(K) Relative ATP levels in LT-HSCs and Lin$^+$ cells sorted from WT and *Srebf1c*$^{-/-}$ mice (n = 5).

(L) Flow cytometric analysis of ROS in MPs, LSKs, and LT-HSCs from WT and *Srebf1c*$^{-/-}$ mice by DCFH-DA staining (n = 5).

(M) Relative lactate levels in LT-HSCs and Lin$^+$ cells sorted from WT and *Srebf1c*$^{-/-}$ mice (n = 5).

*$p < 0.05$, **$p < 0.01$.

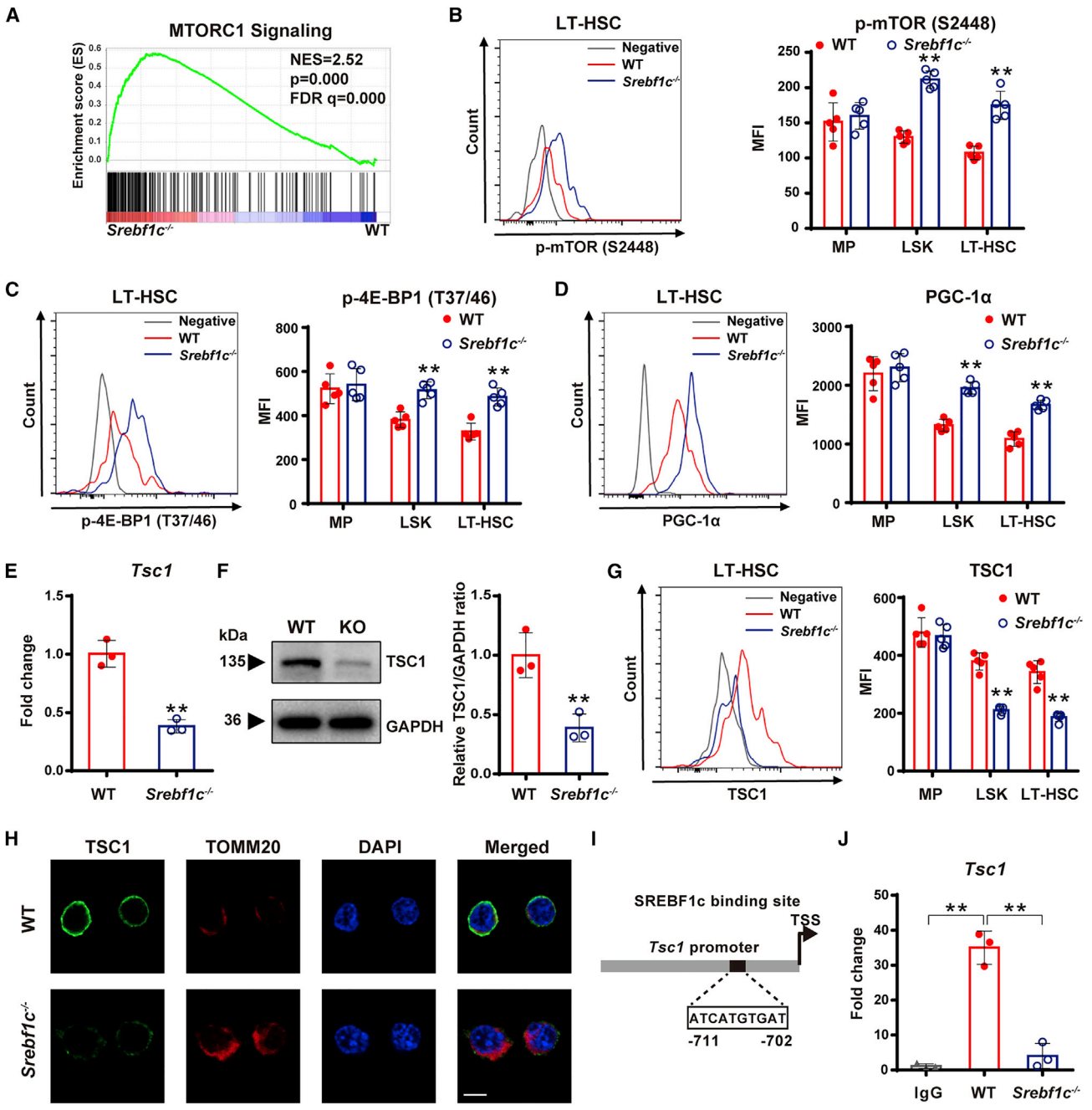

Figure 6. SREBF1c inhibits the hyperactivation of mTOR signaling via the transcriptional control of *Tsc1*

(A) GSEA of mTORC1 pathway in RNA-seq data from WT and *Srebf1c*$^{-/-}$ LSKs.

(B–D) Flow cytometric analysis of the expressions of (B) p-mTOR (S2448), (C) p-4E-BP1 (T37/46), and (D) PGC-1α in MPs, LSKs, and LT-HSCs of WT and *Srebf1c*$^{-/-}$ mice (n = 5).

(E) Quantitative real-time-PCR analysis of *Tsc1* expression in WT and *Srebf1c*$^{-/-}$ LT-HSCs (n = 3).

(F) Western blot analysis of TSC1 protein expression in LSKs sorted from WT and *Srebf1c*$^{-/-}$ mice. Representative Western blot of 3 biological replicates is shown at left and quantitative analysis of the relative TSC1:glyceraldehyde 3-phosphate dehydrogenase (GAPDH) ratio is shown at right.

(G) Flow cytometric analysis of the expression of TSC1 in MPs, LSKs, and LT-HSCs from WT and *Srebf1c*$^{-/-}$ mice (n = 5).

(H) Immunofluorescence staining of TSC1 (green) and TOMM20 (red) in the LT-HSCs sorted from WT and *Srebf1c*$^{-/-}$ mice. Nuclei were stained with DAPI (blue). The scale bar represents 5 μm.

(legend continued on next page)

Mitochondrial mass, mitochondrial membrane potential, ROS levels, and glucose uptake analysis

WT and *Srebf1c*$^{-/-}$ cells were first incubated with HSPC markers. Then, samples were stained with 20 nM Mito Tracker Green (MTG; Thermo Fisher), 20 nM tetramethylrhodamine methyl ester (TMRM; Thermo Fisher), 10 μM 2′,7′-dichlorodihydrofluorescein diacetate (DCFH-DA; Beyotime, Shanghai, China) or 20 μM 2-deoxy-2-((7-nitro-2,1,3-benzoxadiazol-4-yl) amino) (2-NBDG; Thermo Fisher) as previously described (Hu et al., 2018; Mansell et al., 2021).

ATP measurement

ATP measurement was performed as previously described, with minor modifications (Mansell et al., 2021). In brief, 1 × 10^4 LT-HSCs or Lin$^+$ cells sorted from WT and *Srebf1c*$^{-/-}$ mice were resuspended in 100 μL PBS containing 2% fetal bovine serum (FBS), and then transferred into a 96-well plate, followed by the addition of 50 μL detergent and substrate solution. Finally, the ATP level was measured using the Luminescent ATP Detection Assay Kit (Abcam, Cambridge, UK).

Seahorse assays

The OCR and extracellular acidification rate were detected using the Agilent Seahorse XFp Cell Mito Stress Test Kit or the Glycolysis Stress Test Kit (Agilent Technologies, Santa Clara, CA, USA) as previously described (Hu et al., 2018; Rao et al., 2019). Briefly, sorted LSKs (5 × 10^4) were plated into miniplates precoated with CellTak (BD Biosciences). For the Mito Stress Test, cells were suspended in XF assay medium containing 1 mM pyruvate, 10 mM glucose, and 2 mM glutamine (pH 7.4), and then incubated in a CO_2-free incubator at 37°C. Finally, respiration was measured by an Agilent Seahorse XFp analyzer (Agilent Technologies) after sequential addition of 1 μM oligomycin, 1 μM carbonilcyanide p-triflouromethoxyphenylhydrazone (FCCP), and 0.5 μM rotenone/antimycin A (Agilent Technologies). For the glycolysis stress test, cells were suspended in XF base medium supplemented with 1 mM glutamine (pH 7.4) and then incubated in a CO_2-free incubator at 37°C. Finally, the glycolysis stress test was measured by an Agilent Seahorse XFp analyzer after the sequential addition of 10 mM glucose, 2 μM oligomycin, and 50 mM 2-deoxy-D-glucose (2-DG) (Agilent Technologies).

RNA-seq

Transcriptome sequencing was conducted at Shanghai Sinomics (Shanghai, China). In brief, LSKs (1 × 10^5 per sample) were sorted from WT and *Srebf1c*$^{-/-}$ mice by flow cytometry, and total RNA was extracted using the RNAqueous Kit (Ambion, Darmstadt, Germany). Paired-end libraries were synthesized by using the TruSeq RNA Sample Preparation Kit (Illumina, San Diego, CA, USA) following the user manuals. After purification and enrichment, library fragments were loaded into cBot to generate clusters, followed by sequencing on an Illumina NovaSeq 6000. Differentially expressed genes were defined by fold change >2.0 and $p < 0.05$, and then used for Gene Ontology (GO) and Kyoto Encyclopedia of Genes and Genomes (KEGG) pathway enrichment analysis. GSEA was performed using GSEA_4.0.3 software, and gene sets were summarized from previous studies (Cabezas-Wallscheid et al., 2017; Nakagawa and Rathinam, 2018). The sequencing data were submitted to the BioProject database: PRJNA723365.

Statistical analysis

Data analysis was performed using GraphPad Prism 6.0 software (La Jolla, CA, USA). All of the experiments were independently performed at least three times. Unpaired Student's t test (two-tailed) was used for two group comparisons, and one-way ANOVA was used for multiple group comparisons. The log rank test and Kaplan-Meier curve were used for survival analysis. All of the data were shown as the mean ± SD. *$p < 0.05$ and **$p < 0.01$ are depicted as statistically significant differences.

Data and code availability

The data that support the findings of this study are available from the BioProject database: PRJNA723365.

SUPPLEMENTAL INFORMATION

Supplemental information can be found online at https://doi.org/10.1016/j.stemcr.2022.01.011.

AUTHOR CONTRIBUTIONS

Y.L. and Z.Z. designed the study, performed the experiments, analyzed the data, and wrote the paper. S.W., Y.Q., and F.C. performed some animal experiments and analyzed the data. Y.X., M.S., and M.C. participated in some *in vitro* experiments. N.C., L.Y., and S.C. participated in the data analysis. F.W. and Y.S. participated in the initial experimental design and discussed the manuscript. M.H. and J.W. conceived and supervised the study and revised the manuscript.

CONFLICTS OF INTEREST

The authors declare no competing interests.

ACKNOWLEDGMENTS

We thank Prof. Jinyong Wang for the gift of the CD45.1 mice, Yang Liu for technical support in flow cytometry, and Liting Wang for technical support in immunofluorescence microscopy. This work was supported by grants from the National Natural Science Foundation of China (nos. 81930090 and 81725019) and the Scientific Research Project of PLA (AWS16J014).

(I) Schematic diagram of the predicted SREBF1c binding site in the *Tsc1* promoter region.
(J) ChIP-PCR analysis of the binding of SREBF1c to the promoter region of *Tsc1* in WT and *Srebf1c*$^{-/-}$ LSKs. Immunoglobulin G (IgG) served as a negative control.
**$p < 0.01$.

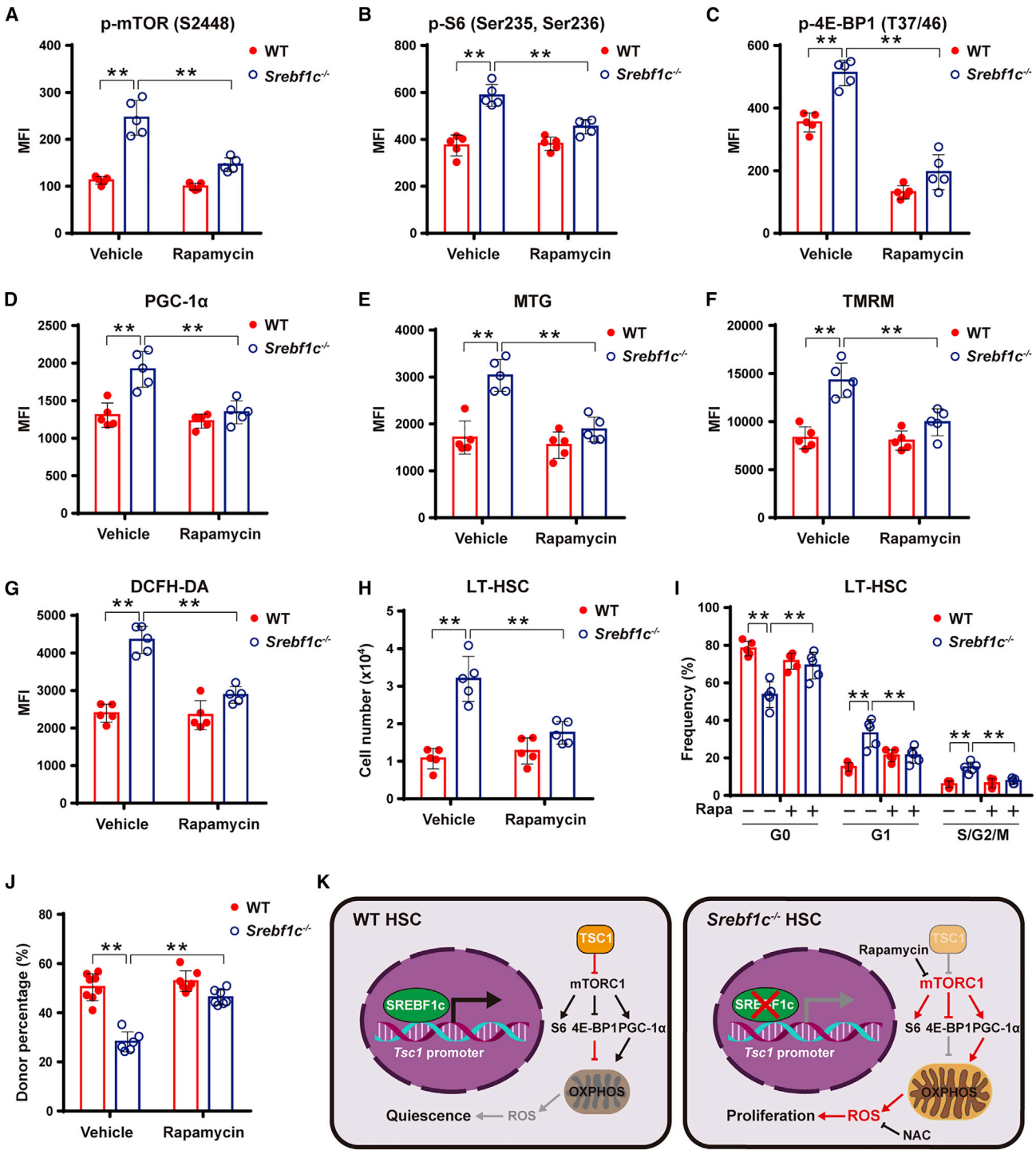

Figure 7. Inhibition of mTOR activation improves HSC defects in *Srebf1c*-deleted mice

(A–I) WT and *Srebf1c*$^{-/-}$ mice were administered intraperitoneally (i.p.) vehicle or rapamycin (4 mg/kg) every other day for 2 weeks. Mean fluorescence intensities (MFIs) of (A) p-mTOR (S2448), (B) p-S6 (Ser235, Ser236), (C) p-4E-BP1 (T37/46), (D) PGC-1α, (E) MTG, (F) TMRM, and (G) DCFH-DA in LT-HSCs from WT and *Srebf1c*$^{-/-}$ mice were analyzed by flow cytometry (n = 5). (H) The absolute number (2 femurs and tibias) and (I) cell-cycle distribution of LT-HSCs from WT and *Srebf1c*$^{-/-}$ mice were analyzed by flow cytometry (n = 5).

(legend continued on next page)

Received: July 10, 2021
Revised: January 13, 2022
Accepted: January 13, 2022
Published: February 10, 2022

REFERENCES

Assmann, N., O'Brien, K.L., Donnelly, R.P., Dyck, L., Zaiatz-Bittencourt, V., Loftus, R.M., Heinrich, P., Oefner, P.J., Lynch, L., Gardiner, C.M., et al. (2017). Srebp-controlled glucose metabolism is essential for NK cell functional responses. Nat. Immunol. *18*, 1197–1206. https://doi.org/10.1038/ni.3838.

Baumgartner, C., Toifl, S., Farlik, M., Halbritter, F., Scheicher, R., Fischer, I., Sexl, V., Bock, C., and Baccarini, M. (2018). An ERK-dependent feedback mechanism prevents hematopoietic stem cell exhaustion. Cell Stem Cell *22*, 879–892.e6. https://doi.org/10.1016/j.stem.2018.05.003.

Cabezas-Wallscheid, N., Buettner, F., Sommerkamp, P., Klimmeck, D., Ladel, L., Thalheimer, F.B., Pastor-Flores, D., Roma, L.P., Renders, S., Zeisberger, P., et al. (2017). Vitamin A-retinoic acid signaling regulates hematopoietic stem cell dormancy. Cell *169*, 807–823.e19. https://doi.org/10.1016/j.cell.2017.04.018.

Cantó, C., Gerhart-Hines, Z., Feige, J.N., Lagouge, M., Noriega, L., Milne, J.C., Elliott, P.J., Puigserver, P., and Auwerx, J. (2009). AMPK regulates energy expenditure by modulating NAD+ metabolism and SIRT1 activity. Nature *458*, 1056–1060. https://doi.org/10.1038/nature07813.

Carrelha, J., Meng, Y., Kettyle, L.M., Luis, T.C., Norfo, R., Alcolea, V., Boukarabila, H., Grasso, F., Gambardella, A., Grover, A., et al. (2018). Hierarchically related lineage-restricted fates of multipotent haematopoietic stem cells. Nature *554*, 106–111. https://doi.org/10.1038/nature25455.

Cermenati, G., Audano, M., Giatti, S., Carozzi, V., Porretta-Serapiglia, C., Pettinato, E., Ferri, C., D'Antonio, M., De Fabiani, E., Crestani, M., et al. (2015). Lack of sterol regulatory element binding factor-1c imposes glial fatty acid utilization leading to peripheral neuropathy. Cell Metab. *21*, 571–583. https://doi.org/10.1016/j.cmet.2015.02.016.

Chen, C., Liu, Y., Liu, R., Ikenoue, T., Guan, K.L., Liu, Y., and Zheng, P. (2008). TSC-mTOR maintains quiescence and function of hematopoietic stem cells by repressing mitochondrial biogenesis and reactive oxygen species. J. Exp. Med. *205*, 2397–2408. https://doi.org/10.1084/jem.20081297.

Cunningham, J.T., Rodgers, J.T., Arlow, D.H., Vazquez, F., Mootha, V.K., and Puigserver, P. (2007). mTOR controls mitochondrial oxidative function through a YY1–PGC-1α transcriptional complex. Nature *450*, 736–740. https://doi.org/10.1038/nature06322.

Filippi, M.D., and Ghaffari, S. (2019). Mitochondria in the maintenance of hematopoietic stem cells: new perspectives and opportunities. Blood *133*, 1943–1952. https://doi.org/10.1182/blood-2018-10-808873.

Gan, B., Hu, J., Jiang, S., Liu, Y., Sahin, E., Zhuang, L., Fletcher-Sananikone, E., Colla, S., Wang, Y.A., Chin, L., and Depinho, R.A. (2010). Lkb1 regulates quiescence and metabolic homeostasis of haematopoietic stem cells. Nature *468*, 701–704. https://doi.org/10.1038/nature09595.

Gan, B., Sahin, E., Jiang, S., Sanchez-Aguilera, A., Scott, K.L., Chin, L., Williams, D.A., Kwiatkowski, D.J., and DePinho, R.A. (2008). mTORC1-dependent and -independent regulation of stem cell renewal, differentiation, and mobilization. Proc. Natl. Acad. Sci. U S A *105*, 19384–19389. https://doi.org/10.1073/pnas.0810584105.

Ghosh, J., Kobayashi, M., Ramdas, B., Chatterjee, A., Ma, P., Mali, R.S., Carlesso, N., Liu, Y., Plas, D.R., Chan, R.J., and Kapur, R. (2016). S6K1 regulates hematopoietic stem cell self-renewal and leukemia maintenance. J. Clin. Invest. *126*, 2621–2625. https://doi.org/10.1172/JCI84565.

Gu, Q., Yang, X., Lv, J., Zhang, J., Xia, B., Kim, J.D., Wang, R., Xiong, F., Meng, S., Clements, T.P., et al. (2019). AIBP-mediated cholesterol efflux instructs hematopoietic stem and progenitor cell fate. Science *363*, 1085–1088. https://doi.org/10.1126/science.aav1749.

Gu, Y., Jones, A.E., Yang, W., Liu, S., Dai, Q., Liu, Y., Swindle, C.S., Zhou, D., Zhang, Z., Ryan, T.M., et al. (2016). The histone H2A deubiquitinase Usp16 regulates hematopoiesis and hematopoietic stem cell function. Proc. Natl. Acad. Sci. U S A *113*, E51–E60. https://doi.org/10.1073/pnas.1517041113.

Hagiwara, A., Cornu, M., Cybulski, N., Polak, P., Betz, C., Trapani, F., Terracciano, L., Heim, M.H., Ruegg, M.A., and Hall, M.N. (2012). Hepatic mTORC2 activates glycolysis and lipogenesis through Akt, glucokinase, and SREBP1c. Cell Metab. *15*, 725–738. https://doi.org/10.1016/j.cmet.2012.03.015.

Hay, N. (2005). The Akt-mTOR tango and its relevance to cancer. Cancer Cell *8*, 179–183. https://doi.org/10.1016/j.ccr.2005.08.008.

Hou, Y., Li, W., Sheng, Y., Li, L., Huang, Y., Zhang, Z., Zhu, T., Peace, D., Quigley, J.G., Wu, W., et al. (2015). The transcription factor Foxm1 is essential for the quiescence and maintenance of hematopoietic stem cells. Nat. Immunol. *16*, 810–818. https://doi.org/10.1038/ni.3204.

Hu, M., Lu, Y., Zeng, H., Zhang, Z., Chen, S., Qi, Y., Xu, Y., Chen, F., Tang, Y., Chen, M., et al. (2021). MicroRNA-21 maintains hematopoietic stem cell homeostasis through sustaining the NF-kappaB signaling pathway in mice. Haematologica *106*, 412–423. https://doi.org/10.3324/haematol.2019.236927.

Hu, M., Zeng, H., Chen, S., Xu, Y., Wang, S., Tang, Y., Wang, X., Du, C., Shen, M., Chen, F., et al. (2018). SRC-3 is involved in

(J) BM cells (1×10^6) from WT or *Srebf1c*$^{-/-}$ mice (CD45.2) coupled with BM cells (1×10^6) from CD45.1$^+$ mice were transplanted into lethally irradiated CD45.1$^+$ recipients. One week after transplantation, recipients received vehicle or rapamycin (4 mg/kg) by i.p. injection every day for 12 weeks. The donor percentages in the recipients' PB were analyzed by flow cytometry (n = 6–8).
(K) Schematic overview of the proposed model demonstrating the role of *Srebf1c* in regulating HSC homeostasis.
**$p < 0.01$.

maintaining hematopoietic stem cell quiescence by regulation of mitochondrial metabolism in mice. Blood *132*, 911–923. https://doi.org/10.1182/blood-2018-02-831669.

Inoki, K., Li, Y., Zhu, T., Wu, J., and Guan, K.L. (2002). TSC2 is phosphorylated and inhibited by Akt and suppresses mTOR signalling. Nat. Cell Biol. *4*, 648–657. https://doi.org/10.1038/ncb839.

Jacinto, E., Loewith, R., Schmidt, A., Lin, S., Ruegg, M.A., Hall, A., and Hall, M.N. (2004). Mammalian TOR complex 2 controls the actin cytoskeleton and is rapamycin insensitive. Nat. Cell Biol. *6*, 1122–1128. https://doi.org/10.1038/ncb1183.

Kalaitzidis, D., Sykes, S.M., Wang, Z., Punt, N., Tang, Y., Ragu, C., Sinha, A.U., Lane, S.W., Souza, A.L., Clish, C.B., et al. (2012). mTOR complex 1 plays critical roles in hematopoiesis and Pten-loss-evoked leukemogenesis. Cell Stem Cell *11*, 429–439. https://doi.org/10.1016/j.stem.2012.06.009.

Khoa, L.T.P., Tsan, Y.-C., Mao, F., Kremer, D.M., Sajjakulnukit, P., Zhang, L., Zhou, B., Tong, X., Bhanu, N.V., Choudhary, C., et al. (2020). Histone acetyltransferase MOF Blocks acquisition of quiescence in ground-state ESCs through activating fatty acid oxidation. Cell Stem Cell *27*, 441–458.e10. https://doi.org/10.1016/j.stem.2020.06.005.

Lee, D.-F., Kuo, H.-P., Chen, C.-T., Hsu, J.-M., Chou, C.-K., Wei, Y., Sun, H.-L., Li, L.-Y., Ping, B., Huang, W.-C., et al. (2007). IKKβ suppression of TSC1 links inflammation and tumor angiogenesis via the mTOR pathway. Cell *130*, 440–455. https://doi.org/10.1016/j.cell.2007.05.058.

Lee, G., Jang, H., Kim, Y., Choe, S., Kong, J., Hwang, I., Park, J., Im, S., and Kim, J. (2019). SREBP1c-PAX4 Axis mediates pancreatic β-cell compensatory responses upon metabolic stress. Diabetes *68*, 81–94. https://doi.org/10.2337/db18-0556.

Li, Z., Qian, P., Shao, W., Shi, H., He, X.C., Gogol, M., Yu, Z., Wang, Y., Qi, M., Zhu, Y., et al. (2018). Suppression of m(6)A reader Ythdf2 promotes hematopoietic stem cell expansion. Cell Res. *28*, 904–917. https://doi.org/10.1038/s41422-018-0072-0.

Liang, G., Yang, J., Horton, J.D., Hammer, R.E., Goldstein, J.L., and Brown, M.S. (2002). Diminished hepatic response to fasting/refeeding and liver X receptor agonists in mice with selective deficiency of sterol regulatory element-binding protein-1c. J. Biol. Chem. *277*, 9520–9528. https://doi.org/10.1074/jbc.M111421200.

Liang, R., Arif, T., Kalmykova, S., Kasianov, A., Lin, M., Menon, V., Qiu, J., Bernitz, J.M., Moore, K., Lin, F., et al. (2020). Restraining lysosomal activity preserves hematopoietic stem cell quiescence and potency. Cell Stem Cell *26*, 359–376.e7. https://doi.org/10.1016/j.stem.2020.01.013.

Liu, L., Inoki, A., Fan, K., Mao, F., Shi, G., Jin, X., Zhao, M., Ney, G., Sun, S., Dou, Y., et al. (2019). ER associated degradation preserves hematopoietic stem cell quiescence and self-renewal by restricting mTOR activity. Blood *136*, 2975–2986. https://doi.org/10.1101/709964.

Ludikhuize, M.C., Meerlo, M., Gallego, M.P., Xanthakis, D., Burgaya Julia, M., Nguyen, N.T.B., Brombacher, E.C., Liv, N., Maurice, M.M., Paik, J.H., et al. (2020). Mitochondria define intestinal stem cell differentiation downstream of a FOXO/notch Axis. Cell Metab. *32*, 889–900.e7. https://doi.org/10.1016/j.cmet.2020.10.005.

Mansell, E., Sigurdsson, V., Deltcheva, E., Brown, J., James, C., Miharada, K., Soneji, S., Larsson, J., and Enver, T. (2021). Mitochondrial potentiation ameliorates age-related heterogeneity in hematopoietic stem cell function. Cell Stem Cell *28*, 241–256.e6. https://doi.org/10.1016/j.stem.2020.09.018.

Mendelson, A., and Frenette, P.S. (2014). Hematopoietic stem cell niche maintenance during homeostasis and regeneration. Nat. Med. *20*, 833–846. https://doi.org/10.1038/nm.3647.

Morita, M., Gravel, S.P., Chenard, V., Sikstrom, K., Zheng, L., Alain, T., Gandin, V., Avizonis, D., Arguello, M., Zakaria, C., et al. (2013). mTORC1 controls mitochondrial activity and biogenesis through 4E-BP-dependent translational regulation. Cell Metab. *18*, 698–711. https://doi.org/10.1016/j.cmet.2013.10.001.

Nakagawa, M.M., and Rathinam, C.V. (2018). Constitutive activation of the canonical NF-kappaB pathway leads to bone marrow failure and induction of erythroid signature in hematopoietic stem cells. Cell Rep. *25*, 2094–2109.e4. https://doi.org/10.1016/j.celrep.2018.10.071.

Norrmen, C., Figlia, G., Lebrun-Julien, F., Pereira, J.A., Trotzmuller, M., Kofeler, H.C., Rantanen, V., Wessig, C., van Deijk, A.L., Smit, A.B., et al. (2014). mTORC1 controls PNS myelination along the mTORC1-RXRgamma-SREBP-lipid biosynthesis axis in Schwann cells. Cell Rep. *9*, 646–660. https://doi.org/10.1016/j.celrep.2014.09.001.

Pinho, S., and Frenette, P.S. (2019). Haematopoietic stem cell activity and interactions with the niche. Nat. Rev. Mol. Cell Biol. *20*, 303–320. https://doi.org/10.1038/s41580-019-0103-9.

Qian, P., He, X.C., Paulson, A., Li, Z., Tao, F., Perry, J.M., Guo, F., Zhao, M., Zhi, L., Venkatraman, A., et al. (2016). The dlk1-gtl2 locus preserves LT-HSC function by inhibiting the PI3K-mTOR pathway to restrict mitochondrial metabolism. Cell Stem Cell *18*, 214–228. https://doi.org/10.1016/j.stem.2015.11.001.

Rao, T.N., Hansen, N., Hilfiker, J., Rai, S., Majewska, J.M., Lekovic, D., Gezer, D., Andina, N., Galli, S., Cassel, T., et al. (2019). JAK2-mutant hematopoietic cells display metabolic alterations that can be targeted to treat myeloproliferative neoplasms. Blood *134*, 1832–1846. https://doi.org/10.1182/blood.2019000162.

Saxton, R.A., and Sabatini, D.M. (2017). mTOR signaling in growth, metabolism, and disease. Cell *168*, 960–976. https://doi.org/10.1016/j.cell.2017.02.004.

Sinha, S., Dwivedi, T.R., Yengkhom, R., Bheemsetty, V.A., Abe, T., Kiyonari, H., VijayRaghavan, K., and Inamdar, M.S. (2019). Asrij/OCIAD1 suppresses CSN5-mediated p53 degradation and maintains mouse hematopoietic stem cell quiescence. Blood *133*, 2385–2400. https://doi.org/10.1182/blood.2019000530.

Su, S., Tian, H., Jia, X., Zhu, X., Wu, J., Zhang, Y., Chen, Y., Li, Z., and Zhou, Y. (2020). Mechanistic insights into the effects of SREBP1c on hepatic stellate cell and liver fibrosis. J. Cell. Mol. Med. *24*, 10063–10074. https://doi.org/10.1111/jcmm.15614.

Suda, T., Takubo, K., and Semenza, G.L. (2011). Metabolic regulation of hematopoietic stem cells in the hypoxic niche. Cell Stem Cell *9*, 298–310. https://doi.org/10.1016/j.stem.2011.09.010.

Takubo, K., Goda, N., Yamada, W., Iriuchishima, H., Ikeda, E., Kubota, Y., Shima, H., Johnson, R.S., Hirao, A., Suematsu, M., and Suda, T. (2010). Regulation of the HIF-1alpha level is essential for

hematopoietic stem cells. Cell Stem Cell *7*, 391–402. https://doi.org/10.1016/j.stem.2010.06.020.

Takubo, K., Nagamatsu, G., Kobayashi, C.I., Nakamura-Ishizu, A., Kobayashi, H., Ikeda, E., Goda, N., Rahimi, Y., Johnson, R.S., Soga, T., et al. (2013). Regulation of glycolysis by pdk functions as a metabolic checkpoint for cell cycle quiescence in hematopoietic stem cells. Cell Stem Cell *12*, 49–61. https://doi.org/10.1016/j.stem.2012.10.011.

Tohyama, S., Fujita, J., Hishiki, T., Matsuura, T., Hattori, F., Ohno, R., Kanazawa, H., Seki, T., Nakajima, K., Kishino, Y., et al. (2016). Glutamine oxidation is indispensable for survival of human pluripotent stem cells. Cell Metab. *23*, 663–674. https://doi.org/10.1016/j.cmet.2016.03.001.

Umemoto, T., Hashimoto, M., Matsumura, T., Nakamura-Ishizu, A., and Suda, T. (2018). Ca(2+)-mitochondria axis drives cell division in hematopoietic stem cells. J. Exp. Med. *215*, 2097–2113. https://doi.org/10.1084/jem.20180421.

Villegas, F., Lehalle, D., Mayer, D., Rittirsch, M., Stadler, M.B., Zinner, M., Olivieri, D., Vabres, P., Duplomb-Jego, L., De Bont, E.S.J.M., et al. (2019). Lysosomal signaling licenses embryonic stem cell differentiation via inactivation of Tfe3. Cell Stem Cell *24*, 257–270.e8. https://doi.org/10.1016/j.stem.2018.11.021.

Wang, H., Diao, D.J., Shi, Z.C., Zhu, X.D., Gao, Y.W., Gao, S.R., Liu, X.Y., Wu, Y., Rudolph, K.L., Liu, G.H., et al. (2016). SIRT6 controls hematopoietic stem cell homeostasis through epigenetic regulation of Wnt signaling. Cell Stem Cell *18*, 495–507. https://doi.org/10.1016/j.stem.2016.03.005.

Wang, N., Yin, J., You, N., Yang, S., Guo, D., Zhao, Y., Ru, Y., Liu, X., Cheng, H., Ren, Q., et al. (2021). TWIST1 preserves hematopoietic stem cell function via the CACNA1B/Ca2+/mitochondria axis. Blood *137*, 2907–2919. https://doi.org/10.1182/blood.2020007489.

Wang, Y., Viscarra, J., Kim, S.-J., and Sul, H.S. (2015). Transcriptional regulation of hepatic lipogenesis. Nat. Rev. Mol. Cell Biol. *16*, 678–689. https://doi.org/10.1038/nrm4074.

Xia, P., Wang, S., Ye, B., Du, Y., Li, C., Xiong, Z., Qu, Y., and Fan, Z. (2018). A circular RNA protects dormant hematopoietic stem cells from DNA sensor cGAS-mediated exhaustion. Immunity *48*, 688–701.e7. https://doi.org/10.1016/j.immuni.2018.03.016.

Yamashita, M., and Passegue, E. (2019). TNF-alpha coordinates hematopoietic stem cell survival and myeloid regeneration. Cell Stem Cell *25*, 357–372.e7. https://doi.org/10.1016/j.stem.2019.05.019.

Yecies, J.L., Zhang, H.H., Menon, S., Liu, S., Yecies, D., Lipovsky, A.I., Gorgun, C., Kwiatkowski, D.J., Hotamisligil, G.S., Lee, C.H., and Manning, B.D. (2011). Akt stimulates hepatic SREBP1c and lipogenesis through parallel mTORC1-dependent and independent pathways. Cell Metab. *14*, 21–32. https://doi.org/10.1016/j.cmet.2011.06.002.